LBL-28738
UC-402

Lawrence Berkeley Laboratory

UNIVERSITY OF CALIFORNIA

Environmental Research Program

1989 Annual Report

Applied Science Division

October 1990

LOAN COPY
Circulates
for 2 weeks
Bldg. 50 Library.
LBL-28738
Copy 2

Available to DOE and DOE Contractors from
Office of Scientific and Technical Information
P.O. Box 62, Oak Ridge, TN 37831
Prices available from (615) 576-8401, FTS 626-8401

Available to the public from
National Technical Information Service
U.S. Department of Commerce
5285 Port Royal Road, Springfield, VA 22161

Prepared for the U.S. Department of Energy under Contract No. DE-AC03-76SF00098

DISCLAIMER

This document was prepared as an account of work sponsored by the United States Government. While this document is believed to contain correct information, neither the United States Government nor any agency thereof, nor the Regents of the University of California, nor any of their employees, makes any warranty, express or implied, or assumes any legal responsibility for the accuracy, completeness, or usefulness of any information, apparatus, product, or process disclosed, or represents that its use would not infringe privately owned rights. Reference herein to any specific commercial product, process, or service by its trade name, trademark, manufacturer, or otherwise, does not necessarily constitute or imply its endorsement, recommendation, or favoring by the United States Government or any agency thereof, or the Regents of the University of California. The views and opinions of authors expressed herein do not necessarily state or reflect those of the United States Government or any agency thereof or the Regents of the University of California.

Environmental Research Program 1989 Annual Report

Tihomir Novakov, *Program Leader*

Applied Science Division
Lawrence Berkeley Laboratory
University of California
Berkeley, California 94720
(415) 486-5001

LBL-28738

LAWRENCE BERKELEY LABORATORY
APPLIED SCIENCE DIVISION

DIVISION DIRECTOR
EJ CAIRNS

DIVISION ADMINISTRATOR
CA FRAGIADAKIS

DEPUTY DIVISION DIRECTOR
DF GRETHER

ASSISTANT DIVISION DIRECTOR
AT QUINTANILHA

DIVISION COUNCIL
EJ CAIRNS, Chairperson

PROFESSIONAL STAFF COMMITTEE
MA WAHLIG, Chairperson

CENTER FOR ATMOSPHERIC AND BIOSPHERIC EFFECTS OF TECHNOLOGY
AT QUINTANILHA, Director

CENTER FOR BUILDING SCIENCE
AH ROSENFELD, Director

ENERGY CONVERSION & STORAGE PROGRAM
EJ CAIRNS, Leader
HW BLANCH, Deputy
MA WAHLIG, Deputy

- **ELECTROCHEMICAL GROUP**
  EJ CAIRNS, Leader
  FR MCLARNON, Deputy
  K KINOSHITA
- **MICROSTRUCTURED MATERIALS GROUP**
  AJ HUNT, Leader
- **BIOTECHNOLOGY**
  HW BLANCH
  CJ KING
  CR WILKE
- **FOSSIL FUELS**
  RH FISH
  S LYNN
- **HIGH T_c SUPERCONDUCTOR PROCESSING**
  PH BERDAHL
  AJ HUNT
  MD RUBIN
  RE RUSSO

ENVIRONMENTAL RESEARCH PROGRAM
T NOVAKOV, Leader
NJ BROWN, Deputy

- **ATMOSPHERIC AEROSOL GROUP**
  T NOVAKOV, Leader
  AD HANSEN
  WH BENNER
- **COMBUSTION GROUP**
  NJ BROWN, Leader
  RK CHENG
  D LUCAS
  AK OPPENHEIM
  RF SAWYER
  L TALBOT
  RB WILLIAMSON
- **MEMBRANE BIOENERGETICS GROUP**
  L PACKER, Leader
  RJ MEHLHORN
  AT QUINTANILHA
- **FLUE GAS CHEMISTRY GROUP**
  SG CHANG, Leader
- **ECOLOGICAL SYSTEMS**
  J HARTE
  SL ANDERSON
- **ANALYTICAL CHEMISTRY**
  F ASARO
  RD GIAUQUE

INDOOR ENVIRONMENT PROGRAM
JM DAISEY, Leader
AV NERO, Deputy

- **INDOOR RADON GROUP**
  WJ FISK, Acting Leader
  RG SEXTRO
  AJ GADGIL
- **INDOOR ORGANIC CHEMISTRY GROUP**
  JM DAISEY, Leader
- **INDOOR AIR QUALITY STUDIES**
  WJ FISK
  GW TRAYNOR
  - VENTILATION
  - CONTROLS
  - EXPOSURE ASSESSMENT
- **ENERGY PERFORMANCE OF BUILDINGS GROUP**
  MH SHERMAN, Leader

ENERGY ANALYSIS PROGRAM
MD LEVINE, Leader
RL RITSCHARD, Deputy

- **ENERGY CONSERVATION POLICY GROUP**
  MD LEVINE, Acting Leader
  JE MCMAHON
  AK MEIER
  I TURIEL
- **BUILDING ENERGY ANALYSIS GROUP**
  RL RITSCHARD, Leader
  H AKBARI
- **INTERNATIONAL ENERGY STUDIES GROUP**
  L SCHIPPER, Co-Leader
  JA SATHAYE, Co-Leader
  AN KETOFF
- **BUILDING ENERGY DATA GROUP**
  JP HARRIS, Leader
- **UTILITY PLANNING & POLICY GROUP**
  EP KAHN, Leader
- **GLOBAL ENERGY/ ENVIRONMENTAL ISSUES**
  MD LEVINE
  WE WESTMAN

BUILDING ENERGY SYSTEMS PROGRAM
MA WAHLIG, Leader

- **BUILDING SYSTEMS ANALYSIS GROUP**
  RC KAMMERUD, Leader
  WL CARROLL
- **SIMULATION RESEARCH GROUP**
  FC WINKELMANN, Leader
- **ABSORPTION HEAT PUMPS**
  JE RASSON
  MA WAHLIG

WINDOWS & LIGHTING PROGRAM
SE SELKOWITZ, Leader

- **WINDOWS & DAYLIGHTING GROUP**
  SE SELKOWITZ, Leader
  JH KLEMS, Deputy
  MD RUBIN, Deputy
  CM LAMPERT
  - OPTICAL MATERIALS
  - FENESTRATION PERFORMANCE
  - BUILDING APPLICATIONS
- **LIGHTING SYSTEMS RESEARCH GROUP**
  SM BERMAN, Leader
  RR VERDERBER, Deputy
  DD HOLLISTER
  DJ LEVY
  - LAMP TECHNOLOGY
  - IMPACTS
  - LIGHTING CONTROLS

April 1990

Program Staff

Tihomir Novakov, *Program Leader*
Nancy J. Brown, *Deputy Program Leader*

Susan Anderson
Frank Asaro
Henry Benner
Nancy Brown*
Johnny Chang
Shih-Ger Chang*
Robert Cheng
Raymond Dod
Ofodike Ezekoye
Carlos Fernandez-Pello
Charles Fleischman
Stephanie Frolich
Ian Fry
Robert Giauque
Gloria Gill
Ralph Greif
Anthony Hansen
John Harte
Erika Hoffman
Kenneth Hom
Minh Hua
Gary Hubbard
Margaret Huflejt
Franklin Hurlbut
David Littlejohn
David Liu
Jua-Huai Lu
Donald Lucas
Robert Macey
John Maguire
Julieta Marcelino
Samuel Markowitz
Richard Martin
Andrew Maxson
Rolf Mehlhorn
Harvey Michaels
Helen Michel
Katherine Moore
Antoni Oppenheim
Lester Packer*
Patrick Pagni
Ahmed Rashed
Chang Woo Rhee
Robert Risebrough
Robert Sawyer
Frank Schipperijn
Richard Schmidt
Richard Schneider
Ian Shepherd
Linda Sindelar
Martyn Smith
David Steward
Lawrence Talbot
Chang-Lin Tien
Derek Watry
Gillian Wild
Robert Williamson
Linda Wroth

*Group Leader

Table of Contents

Introduction i

COMBUSTION
Controlled Combustion 1
Smoke Emission Measurements from Medium-Scale Experiments 2
Thermal Destruction of Toxic Compounds 3
Combustion Chemistry 4
Combustion Fluid Mechanics 5

FLUE-GAS CHEMISTRY
Using Aqueous Mixtures of Yellow Phosphorus-Limestone for Simultaneously Removing SO_2 and NO_x From Flue Gas: Bench-Scale Tests 7
Oxidation of Phosphorous Acid by Nitric Acid 8
Developing Advanced Metal Chelates for Removal of NO from Flue Gas 9
The Isomers and Dimer of Bisulfite Ion 10

ATMOSPHERIC AEROSOLS
Anomalous SO_2 Oxidation in Laboratory Clouds 11
Chemical Characterization of Local and Saharan Dust in the Puerto Rican Atmosphere 12
High-Velocity Impacts With Submicron-Sized Particles 13

ECOLOGICAL SYSTEMS
Predicting Chronic Toxicity in Aquatic and Terrestrial Ecosystems 14

MEMBRANE BIOENERGETICS
Detecting and Preventing Biological Free-Radical Damage 15

ANALYTICAL CHEMISTRY
Asteroid Impacts on the Earth 16

Introduction

The objective of the Environmental Research Program is to contribute to the understanding of the formation, mitigation, transport, transformation, and effects of energy-related pollutants on all compartments of the environment. This multidisciplinary program includes both basic and applied research in physics, chemistry, engineering, ecology, and biology, as well as research and development of advanced technologies for pollutant abatement and destruction, efficient combustion, and new methods of detection and analysis of different contaminants. The Program's Annual Report contains summaries of research performed during 1989 in the areas of combustion, flue-gas chemistry, atmospheric aerosols, ecological systems, membrane bioenergetics, and analytical chemistry.

The *Combustion Group* studies complex combustion processes by acquiring a fundamental understanding of the physical and chemical processes that determine the combustion efficiency, formation, and emissions of species from these processes. The *Flue-Gas Chemistry Group* is engaged in research whose aim is to help develop new processes for simultaneous SO_2 and NO_x removal. The *Atmospheric Aerosols Group* studies atmospheric chemical processes in the laboratory and in the field, and develops novel methods for individual particle characterization. New activities have been initiated by the *Ecological Systems Group* to develop means of predicting the toxicity of contaminants in aquatic and terrestrial ecosystems. The *Membrane Bioenergetics Group* studies the effects of chemically reactive compounds on biological systems. The main emphases in *Analytical Chemistry* have continued to be in the area of asteroid impacts and mass extinctions.

— Combustion—

Controlled Combustion

K. Hom, J.A. Maxson, A.K. Oppenheim, and H.E. Stewart

Current technological standards treat combustion chambers for prime movers solely as sources of power, without much attention being given to their performance as chemical reactors. Consequently, these chambers have a relatively unconstrained tendency to produce air pollutants. In the automotive industry, for example, the strategy adopted worldwide for reducing pollutant emissions has been to reduce their concentrations by chemical processing of combustion products in the exhaust system. In contrast, the basic purpose of our studies is to provide a scientific basis for *controlling the combustion process* in order to reduce formation of pollutants. Notably, the same means benefit fuel economy as well as engine tolerance to a wide variety of fuels.

Our ultimate goal is to advance the technology of internal combustion engines. For this purpose, we must not only understand systems and processes currently in use; we must also explore and assess other concepts. After more than a decade of studying the fundamentals of ignition and combustion—of particular relevance to internal combustion engines—we are now beginning to develop and study new concepts.

Thus, having published studies demonstrating the influence of dilution upon auto-ignition, we have concentrated on developing effective means for executing the combustion process. The major function of these methods is to modify the progress of evolution of exothermic energy and its deposition in the working substance, so as to render it externally controllable by a microprocessor. The particular mode we are exploring in this connection is associated with the use of turbulent plumes of pulsed jets (i.e., pulsed-jet combustion, PJC).

This year we applied for three U.S. patents—one concerning the general features of the method and system for controlled combustion engines, one for a pulsed-jet generator for premixed charge systems such as gasoline engines, and one for a pulsed-jet combustion generator for non-premixed charge systems such as diesel engines.

The primary purpose of our preliminary investigation of PJC was to compare the performance of this mode of combustion to that of a conventional spark-ignited flame traversing the charge (FTC). Using a highly diluted air/fuel mixture as the working substance, we conducted experiments in a constant-volume vessel of a size representative of typical automotive engines in the course of the exothermic process of combustion. Our results showed the advantages of PJC over FTC in initiating and carrying out the combustion process. In particular, they led to the following conclusions:

- *PJC can initiate and promote the combustion process in extremely lean media*, i.e., in a mixture whose equivalence ratio is 0.45. (Under identical conditions, spark ignition requires equivalence ratios under 0.65 in order to initiate combustion.)
- *The effectiveness of a PJC-initiated process is superior to that of FTC*. The PJC rate is about twice as fast and the heat transfer losses to surroundings significantly lower than with FTC, so that the maximum pressure attained in the combustion chamber is about 10% higher.

Future studies will attempt to determine the mechanical and chemical structure of PJC, establishing its properties as a means of executing combustion under microprocessor control so as to restrain formation of pollutants.

References

Lucas D, Cavolowsky JA, Breber PR, Oppenheim AK. Pulsed plasma jet igniters: Species measurements in methane combustion. In: Twenty-Second Symposium (International) on Combustion, Pitttsburgh, PA: The Combustion Institute, 1989, pp. 1661-1667.

Lutz AE, Kee RJ, Miller JA, Dwyer HA, Oppenheim AK. Dynamic effects of autoignition centers for hydrogen and C1, 2-hydrocarbon fuel. Twenty-Second Symposium (International) on Combustion. Pitsburgh, PA: The Combustion Institute, 1989, pp. 1683-1693.

Lutz AE, Oppenheim AK. The effects of product dilution on autoignition in hydrogen and methane. Western States Section Meeting, The Combustion Institute. 1989; .

Oppenheim AK, Beltramo J, Faris DW, Maxson JA, Hom K, Stewart HE. Combustion by pulsed jet plumes—key to controlled combustion engines. SAE Paper 890153, 1989; 10 pp.

Oppenheim AK. Pulsed jet plume combustion—an exothermic process under fluid mechanical control. In: *Twelfth Canadian Congress of Applied Mechanics, Carleton University, Ottawa, Ontario.* 1989; 736-737.

Smoke Emission Measurements from Medium-Scale Experiments

R.B. Williamson, R. Dod, C.M. Fleischmann, N.J. Brown, and T. Novakov

The concept of a "nuclear winter" has been postulated using a number of assumptions regarding the smoke produced by post-nuclear exchange fires. Knowledge of the quantity and character of the smoke emitted by those fires is crucial for predicting their climatic impact.

To help quantify the smoke which might be generated after use of nuclear weapons—and which may cause a "nuclear winter"—we conducted a series of medium-scale fire experiments using representative urban fuels such as wood, asphalt roofing, and liquid petroleum.

More than 20 medium-scale experiments have been conducted in this research program. During each experiment, the mass smoke was determined by sampling the aerosol particulates in the exhaust duct, which captured the effluent from the burning material; the rate of heat release (RHR) was measured by oxygen depletion calorimetry (ODC). In addition, the characteristics of the smoke—particularly its graphitic ("black") carbon content—were analyzed. An important, unique aspect of this research is that some experiments were conducted with limited ventilation by burning materials in a compartment having only a window to admit air inside.

The smoke emission factors measured for wood burning under well-ventilated conditions ranged from 0.1% to 0.3%; under limited conditions, however, this value increased an order of magnitude, i.e., to between 1% and 3%.

For No. 2 fuel oil, the well-ventilated smoke emission factor ranged from 8% to 10% but dropped to 5% when the oil was burned in the compartment. This experiment was not "ventilation-limited"; approximately twice as much oxygen was present than would have been necessary for burning all the fuel volatilized per unit of time. This decrease in emission factor for the oil burned in the compartment is probably attributable to the higher temperature resulting from radiative feedback in the compartment (as compared with the open pan fire) and to more complete combustion resulting in substantial soot burnout.

A burn pan one meter in diameter has been fabricated, and initial experiments have been conducted. Optical smoke measurements using a laser apparatus are being developed, and initial experiments have been conducted.

In the context of a "nuclear winter," the implications of our measurements are centered around four concepts. First, ventilation has a substantial effect on smoke production from burning wood and oil; measured under limited ventilation conditions, the emission factors for wood were more than an order of magnitude higher than those measured under well-ventilated conditions. More importantly, the smoke in the compartment fire was thick and black—similar in appearance to the smoke produced by burning plastic or oil. Wood is one of the major building and furnishing materials used in the United States, and we may reasonably assume that large quantities of wood would burn under both limited and unlimited ventilation conditions in the post-nuclear environment.

Second, the well-ventilated medium-scale wood experiments produced several orders of magnitude more black carbon than did previously reported bench-scale experiments. The black carbon particles absorb sunlight and produce the "nuclear winter" effects.

Third, the smoke emission factors for asphalt roofing shingles (totalling more than 12%, 90% being black carbon) could have a significant impact on urban smoke production in the post-nuclear environment.

Fourth, our experimental results to date show an important trend: the smoke emission factors for oil are decreased as fire size or intensity is increased. The smoke emission factors were more than 10% for the single-pan experiments but decreased when the fire was doubled or placed in the compartment.

We plan to continue our experiments, studying increasing rates of heat release under various ventilation conditions in order to evaluate the effects of scaling. In particular, we will emphasize the study of scaling between our experiments and will explore ways of correlating our findings with those of other investigators.

References

Williamson RB, Fleischmann CM, Dod RL, Brown NJ, Novakov T, Mowrer FW. The use of medium-scale experiments to determine smoke characteristics. *In:* Hasegawa HK, ed. *Characterization and Toxicity of Smoke. ASTM Special Technical Publication No. 1082.* Philadelphia: American Society for Testing and Materials (in press, 1990).

Brown NJ, Dod RL, Mowrer FW, Novakov T, Williamson RB. Smoke emission factors from medium-scale fires. Part I. *Aerosol Science and Technology* 1989; 10:2-19.

Dod RL, Brown NJ, Mowrer FW, Novakov T, Williamson RB. Smoke emission factors from medium-scale fires. Part II. *Aerosol Science and Technology* 1989; 10:20-27.

Thermal Destruction of Toxic Compounds

D. Lucas, R.F. Sawyer, C.P. Koshland, E.M. Fisher, M.J. Hall, and K. Taga

Incinerators currently treat about 1% of the hazardous wastes produced in the United States; this percentage will probably increase as standards for other disposal techniques become more stringent. Each incinerator must demonstrate the capability of destroying 99.99% of the waste that it processes. Normally this goal can be met, but a variety of failure modes and poor operating conditions can lead to formation of undesirable combustion byproducts (known as products of incomplete combustion, or PICs) or to reduced destruction efficiency. These failure modes provide a monitoring and regulatory challenge because of the extreme difficulty of predicting which products will be formed during the combustion of a given waste material. In addition, few methods can detect these products rapidly at low, but potentially dangerous, concentrations.

We have recently begun a study concerned with waste destruction and PIC formation from chlorinated hydrocarbons during deviations from optimal combustion conditions. The research is a combination of experimental and modeling studies. A turbulent-flow reactor (located on the campus of the University of California, Berkeley) can simulate several failure modes, including cool-wall impingement, poor mixing, transients, and poor atomization of droplets. The reactor is coupled to a Fourier transform infrared spectrometer (FTIR) with a multi-pass gas cell to measure most of the important species over a wide range of concentrations. Reactions in the combustor are modeled using the CHEMKIN programs with the SENKIN driver package. We are testing different reaction mechanisms developed for chlorinated hydrocarbon incineration, as well as producing our own mechanism. We are also developing new *in situ* diagnostic methods for chlorinated hydrocarbons using photofragmentation and laser-induced fluorescence. Virtually all chlorinated hydrocarbons absorb UV radiation at excimer laser wavelengths of 193 or 248 nm. Fragments produced from the photodissociation can then fluoresce, either by further absorption from the pump laser beam or induced by another tunable laser beam.

Results of ethyl chloride incineration have shown that substantial quantities of toxic compounds such as vinyl chloride can be produced, and that existing reaction mechanisms do not predict its formation. Infrared spectroscopy has proven to be useful in quantifying products, and the laser-based methods show promise in producing fragments that can be attributed to ethyl chloride.

Combustion Chemistry

N.J. Brown, J. Chang, R.J. Martin, and D. Lucas

We have completed our research on the gas-phase combustion chemistry of N_2O in $H_2/O_2/Ar$ mixtures, and a second study concerned with analyzing and modeling nitrous oxide chemistry in lean, premixed combustion has also been completed. Laminar-flame and homogeneous combustion modeling calculations were performed using the PREMIX and CHEMKIN codes, respectively. Four systems containing H_2, O_2, Ar and an N-containing dopant (NH_3, NO, or N_2O) were modeled and compared to recent flat-flame burner experiments. Agreement between measured and computed N_2O, NO and N_2 concentration profiles indicated that the model is a reasonable representation of the kinetics and transport in the flame system. The effects of assumed burner temperature, temperature profile shaped, mass diffusion, and probing were investigated. A sensitivity analysis of the flame modeling revealed much about the formation and destruction chemistry of N_2O.

For cases where burner temperatures were identical but temperatures were either determined by solving the energy equation numerically or were specified to be equivalent to measured temperatures, calculated N_2O, NO and N_2 profiles differed by 2-15%. Calculations which differed only in specified flame-holder surface temperature (400-1000 K) produced concentration profiles which varied by approximately 20% in NO and N_2, and by as much as a factor of 7 in N_2O. Computations performed with and without mass diffusion showed that profile shapes and final, post-flame concentrations of N_2O, NO and N_2 differed by factors of 1.5 to 3.0 because of the fast transport of low-mass, reactive species. A probe-quench simulation indicated that sampling may alter the N_2O concentration in gases extracted very near the burner surface, but that relatively little species interconversion takes place at heights greater than 1 mm.

Reaction rate and sensitivity results from these computations indicates that the principal formation and destruction reactions for N_2O are

$$NH + NO = N_2O + H$$
$$H + N_2O = N_2 + OH$$

and that

$$H + O_2 + M = HO_2 + M$$

plays a significant role in trapping H atoms to enhance N_2O survival.

Flash-ignited combustion was initiated in a closed quartz cell and was studied with molecular-beam mass spectrometry. A mixture of $NH_3/H_2/O_2/Ar$—where NH_3 was the primary photolysis absorber and the major fuel species—burned inhomogeneously in a confined cell. Concentration profiles of N_2, NO, O_2, and N_2O were derived from the recorded mass signals by correcting for beam overrun and by calibration to known species signals. The final O_2 concentration agreed well with that predicted for complete combustion. Post-flame NO and N_2 concentrations were higher than values previously reported by other investigators for NH_3 flames, but the ratio of these concentrations agreed well with the earlier results. The N/O ratio in reactants is more important than flame pressure or confinement in determining product distributions. A small amount of N_2O was present in the reactant and disappeared during combustion. In reactant mixtures containing NH but not N_2O, no observable combustion-induced increase was seen in the mass 44 signal.

Functional sensitivity analysis was used to study the effects of higher-order terms in HD + HD potential energy surface expanded in the form $V = V(R)_{m1m2} \cos(m1\Phi + m2\Phi)$ on rotational and translational energy transfer. Terms for $m1 \leq 6$ and $m2 \leq 6$ are being considered. Relatively large sensitivities of the energy transfer observables to terms as high as m1 = 6 or m2 = 6 were observed. The main conclusions from preliminary analysis of the sensitivity plots are still in accord with those of our previous work. The results of this new study are currently being analyzed.

In collaboration with Professors Herschel Rabitz (of Princeton University) and Robert Wyatt (of the University of Texas, Austin), we have initiated a new study on the sensitivity of the $F + H_2$ 3-D quantum reactive scattering to two potential energy surfaces. This will be our major research focus for the next year.

References

Martin RJ, Brown NJ. Nitrous oxide formation and destruction in lean premixed combustion. *Combustion and Flame* (in press, 1989; also published as Lawrence Berkeley Laboratory Report No. LBL-27128)

Martin RJ, Brown NJ. Analysis and studies of nitrous oxide chemistry in lean premixed combustion. *Combustion and Flame* (in press, 1989; also published as Lawrence Berkeley Laboratory Report No. LBL-27128)

Brown NJ. Rate coefficient calculations for combustion modeling. *Prog. Astronaut. Aeronaut.* (in press, 1989; also published as Lawrence Berkeley Laboratory Report No. LBL-27097)

Judson RS, Rabitz H, Brown NJ. A classical functional sensitivity analysis of coplanar inelastic scattering for $H_2 + H_2$ and its isotopic analogues. J. Phys. Chem. 1989; 93:2400-2411.

Combustion Fluid Mechanics

R.K. Cheng, I.G. Shepherd, and L. Talbot

Because fluid mechanical turbulence enhances burning rate, turbulent combustion is the dominant mode of operation in most engines and burners. The coupling between turbulence and combustion chemistry is very complex, and the interactions involve significant spatial and time-related fluctuations of temperature, velocity and pressure. These fluctuations affect reaction rate as well as the concentrations of combustion products in the exhaust. Moreover, because the range of chemical and fluctuation time scales span many orders of magnitude, experimental studies and the development of turbulent combustion theory present major challenges to combustion scientists today.

One of the best ways to understand the controlling physical interactions of turbulent combustion is by investigating the combustion flowfields in laboratory-scale burners. The experiments are designed to investigate the regime where the time scales associated with fluid mechanics are large compared with those of chemical reactions so that theoretical treatment of the combustion chemistry can be simplified. Laser diagnostic techniques to measure scalar and velocity fluctuations and statistical cross-correlations produce the data used for comparing and evaluating current theoretical models and for determining the effects of turbulence intensity on burning rates.

For studies of premixed turbulent combustion where the fuel and the oxidizer are thoroughly mixed before combustion, we use three laboratory burners of different geometries: rod-stabilized "v" flames; large, conical tube-stabilized flames of the Bunsen type; and a planar flame stabilized in the stagnation flow. The burners are designed to provide the closest approximation to the idealized flowfield specified by current one-dimensional or two-dimensional theoretical models. In these laboratory flames, the flame sheet or laminar flamelet model provides a good physical description of the flame/flowfield interaction.

When the chemical reactions are confined within flame sheets typically about 1 mm thick, the turbulent scalar field can be specified by considering only the burned and the unburned states. This approximation is valid because the contribution from the flame sheet to the mean scalar quantities is low. The flamelet or flame-sheet model also indicates that the turbulent burning rate is proportional to the increase in the flame area because turbulence wrinkles and corrugates the flame sheet.

In 1989, we developed a high-speed tomographic technique to measure directly the flame area, its length scales, and burning rate. Previously, we had reported on our study that determined burning rate from the flame crossing frequencies measured at points along mean flowlines.

For premixed turbulent combustion and in turbulent flow studies, tomographic technique is a flow-visualization method that provides instantaneous two-dimensional, cross-sectional images of the turbulent flowfield. The technique is based on photographing the flow pattern, visualized by illuminating by a sheet of laser light micron-size seed particles that have been introduced into the flow. The thickness and height of the laser beam define the depth of field and the field of view. For premixed turbulent flames, we use seed particles that evaporate at the flame sheet so that the instantaneous flame surface is marked as the boundary between light regions (representing cold reactants with seed particles) and dark regions (representing hot products without particles) regions on the tomographic record. The light source used in our system is a recently acquired Metalaser copper vapor laser, which delivers 5-mJ pulses of energy with 20-30 nsec pulse width and has a variable repetition rate up to 10 kHz. Using this laser source, we can resolve temporally the instantaneous flame surface and follow the evolution of the flame with time. Tomographic images from the laser pulses are recorded at 4 kHz by a high-speed 16-mm Fastax camera. Film is a convenient and economic means of recording the large amount of data necessary for statistical analysis.

To obtain the record shown in Figure 1, the laser sheet is directed perpendicular to the rod stabilizer and is positioned at the midsection of the flame at 50 mm above the rod. The two wrinkled flame surface boundaries forming the "v" are marked by the white line. The positions of the flame boundaries are deduced using an edge-finding algorithm on the digitized image obtained by a video camera. The flame surface boundaries obtained from at least 200 frames for each movie are analyzed and averaged to infer the large and small flame wrinkle scales (which can be compared to those of turbulence length scales) and to estimate the increase in burning rate.

To deduce the characteristic wrinkle scales for the premixed turbulent flame, the flame boundaries are analyzed by the fractal method. However, unlike typical fractal surfaces whose areas increase continuously with decreasing measur-

Fig. 1. Instantaneous flame boundaries of a turbulent, rod-stabilized "v" flame.

ing scales, these flame boundaries have two additional parameters—the inner and outer cut-off measuring scales corresponding to the smallest and largest flame wrinkle scales. The results show that the fractal dimension of these boundaries, which can be interpreted as the rate at which the surface area increases with the measuring scale, are lower than those obtained for non-reacting isotropic turbulence. The inner and outer cut-offs are about 2.0 mm and 16.0 mm. The inner cut-off is about the same as the integral length scale of the incident turbulence. The ratio of lengths of the boundaries at the the inner and outer cut-offs can also be used to estimate the burning rate. It was found that this ratio was not directly proportional to the burning rate obtained from the flame crossing method. Further analysis has shown that the effects of flow divergence may have to be included in the analysis if the two measurements are to be consistent.

The high-speed tomographic technique is also applied to study turbulent non-premixed (diffusion) jet flames of two different configurations. In non-premixed flames, mixing and burning of the fuel and oxidizer occur simultaneously. Both experiments use a fuel jet with co-flow or opposed flow of air. Figure 2 is an example of a tomographic image obtained for the opposed jet diffusion flame. Because the flowfield consists of mixing and reaction between fuel and air streams, seed particles are introduced into both streams and the reaction zone is shown by the wrinkled dark band with swirls. As can be seen, the tomographic surfaces are different than those of premixed flames; however, these surfaces do not have the same physical significance as those of the premixed flames, and the wrinkles are not related to the reaction rate but indicate the flame stretch induced by turbulence.

In addition to our experimental efforts, we have progressed in our numerical study of premixed turbulent flames using the vortex dynamic technique. The numerical work complements the experimental studies, e.g., by improving the algorithm for describing the flame movements. The flame movement within the reaction zone consists of two components: the first is associated with the convection of the flame by the mean flow, and the second results from flame propagation. Because flame propagation represents the rate at which reactants are converted into products, it is directly related to the burning rate. Previous algorithms assume that the flame propagates everywhere at a constant burning speed. This technique cannot consider the effects of flame curvature or the effects of flame cusps. A new flame movement algorithm (developed by Prof. J. Sethian) for vortex dynamic simulations of premixed turbulent flames is capable of overcoming these limitations, and we have incorporated this algorithm into the numerical program for the "v" flames. The evolution of the shape of the flame interface predicted by this model is compared with those obtained experimentally by tomography. Also deduced from the numerical results are conditioned velocity statistics that can be used to predict flame-generated turbulence.

Fig. 2. Tomographic image obtained for the opposed jet diffusion flame.

— *Flue-Gas Chemistry* —

Using Aqueous Mixtures of Yellow Phosphorus and Limestone for Simultaneously Removing SO_2 and NO_x from Flue Gas: Bench-Scale Tests

D.X. Shen, D. Littlejohn, and S.G. Chang

Previously, we found that aqueous mixtures of yellow phosphorus and limestone could effectively remove SO_2 and NO_x from flue gas. Oxidation of phosphorus generates ozone, which converts NO into more soluble NO_2. The experiments were carried out in a bubbling absorber column 5 cm in diameter, using 200 ml of reaction mixture. The gas flow rate was about 1 liter per minute, corresponding to a superficial velocity of flue gas 0.028 feet per second in the absorption column and the contact time of flue gas with scrubbing liquors of approximately 12 sec. However, in a commercial scrubber system, the superficial velocity of flue gas is much faster (4-12 feet per second) and the contact time much shorter (0.25-5 seconds). Consequently, the mass transfer and chemical reaction kinetics are less favorable under the conditions of a commercial system.

To determine whether the new additives are effective at realistic conditions, we constructed a 600-liter-per-minute bench-scale scrubber system that simulates the conditions of a commercial system. The bench-scale system uses a column 10 cm in diameter and 120 cm long as an absorber. Two types of absorber were constructed—one containing spray nozzles to simulate a conventional spray tower absorber, and the other simulating a Chiyoda bubbling absorber. (The Chiyoda absorber was designed by George Lee of Bechtel Corporation.) The flue gas enters the Chiyoda absorber downward through impingers that submerge 25 cm under the scrubbing liquor. The superficial velocity is about 4 feet per second, and the contact time is about 0.2 seconds. (These values are typical of a commercial Chiyoda-121 scrubbing system.) A simulated flue gas mixture with about 5% oxygen was prepared by mixing evaporated liquid nitrogen with compressed air. NO, SO_2, and CO_2 were blended into the mixture and heated to about 150°C before flowing into the scrubbing system.

We studied the removal efficiency of NO and SO_2 as a function of L/G (the ratio of the flow rate of scrubbing liquor to the flow rate of flue gas) as well as the weight percent of phosphorus and limestone in scrubbing liquors. We found that more than 90% NO removal efficiency can be achieved with a L/G > 60 (gal/min)/(1000 cu ft/min) and a scrubbing liquor containing 0.75% by weight of yellow phosphorus (Figure). In a typical wet limestone flue gas desulfurization system, L/G is typically in the range of 60-120 to achieve 90% SO_2 removal efficiency. The stoichiometric ratio, (P/NO), which represents the effectiveness of phosphorus utilization, was determined to be in the range of 0.6-1.5 under the conditions tested. A mass balance study is in progress, and field tests are planned.

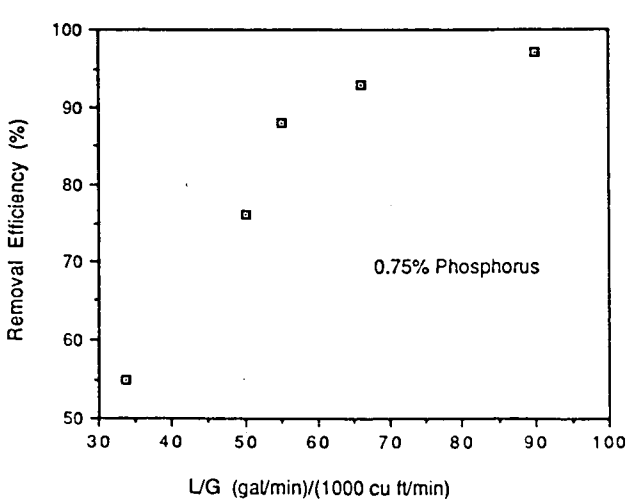

Figure. Efficiency of NO removal for 0.75% phosphorus mixture, expressed as a function of L/G (the ratio of flow rate of scrubbing liquor to flow rate of flue gas).

Reference

Chang SG, Liu D. Removal of Nitrogen and Sulfur Oxides from Waste Gas using a Phosphorus/Alkali Emulsion. Nature 1990; 343: 151. (Also published as Lawrence Berkeley Laboratory Report No. LBL-27373)

Oxidation of Phosphorous Acid by Nitric Acid

Y.Z. Wang and S.G. Chang

The phosphorus-based chemistry for removing NO_x generates finely-divided H_3PO_4 aerosols in the exhaust gas stream; the aerosol can be removed by passing the exhaust gas through phosphoric acid. We sampled the aerosol generated in our experiments by drawing some of the exhaust gas through a filter. The material was analyzed by ion chromatography and its composition was found to be 1.5% H_3PO_2 (hypophosphorous acid), 15% H_3PO_3 (phosphorous acid), and 83.5% H_3PO_4 (orthophosphoric acid).

To generate a commercially usable product, a method is needed for oxidizing the lower phosphorus oxide-based acids to o-phosphoric acid. Dissolved NO_2 from the scrubbing process generates nitric acid, an oxidizing agent. We decided to investigate the oxidation of phosphorous acid by nitric acid.

This reaction is characterized by an induction period during which NO accumulates. The reaction demonstrated a first-order dependence on H_3PO_3 and fourth-order dependence on HNO_3. During the reaction, the concentration of NO_2 first increases, then decreases (Figure).

The effect of the concentration of NO, NO_2^-, H_3PO_3, HNO_3, and Cl^- (ionic strength) on the reaction rate were studied, and the results are summarized below.

NO: Bubbling NO through the reaction mixture eliminated the induction period and increased the rate of the reaction. To determine the effect of NO on the reaction rate, rapid gasflows containing 27%, 53%, and 80% NO were passed through a rapidly stirred solution. The reaction rate showed first-order dependence on NO (rate-order dependence on NO was 1.4). The addition of O_2 to the gas mixture of NO + N_2 that was bubbled through the reaction solution had no effect on the reaction rate. Increasing the gasflow rate reduced the induction period.

NO_2^-: No oxidation of H_3PO_3 occurred at pH 1 to 2. Under more acidic conditions, the reaction proceeded and was proportional to the concentration of NO_2^-.

H_3PO_3: With concentrations of the other reagents held constant, the initial concentration of H_3PO_3 was varied from 0.16 M to 0.55 M. Reaction rate showed first-order dependence on concentration of H_3PO_3.

NO_3^-: The added concentration of NO_3^- was varied over a range of 2 to 4 M, and the rate of reaction displayed first-order dependence on the concentration of NO_3^-. (rate-order dependence on NO_3^- was 1.2).

Cl^- (ionic strength): The Cl^- concentration was varied from 0.25 to 1 M, with the reaction rate increasing with increasing concentration of Cl^-. From the Debye-Huckel theory, this would be expected from a reaction of two species with the same type of charge. In this case, we would expect involvement of species with negative charges.

A possible mechanism for the reaction is as follows. The induction period results from the time necessary for accumulating NO by the following reaction process:

$$2HNO_3 + H_3PO_3 \rightarrow 2NO_2 + H_2O + H_3PO_4$$
$$2NO_2 + H_2O \rightarrow HNO_2 + HNO_3$$
$$2HNO_2 \rightarrow NO + NO_2 + H_2O$$

net:

$$HNO_3 + H_3PO_3 \rightarrow H_3PO_4 + 0.5NO + 0.5NO_2 + 0.5H_2O$$

Then,

$$HNO_3 + NO \rightarrow HN_2O_4^*$$
$$2HN_2O_4^* + H_3PO_3 \rightarrow H_3PO_4 + 2NO_2 + H_2O + 2NO$$
$$2NO_2 + H_2O \rightarrow HNO_2 + HNO_3$$
$$2HNO_2 \rightarrow NO + NO_2 + H_2O$$

net:

$$HNO_3 + H_3PO_3 + 2NO \rightarrow H_3PO_4 + 2.5NO + 0.5NO_2 + 0.5H_2O$$

The determination of a reaction rate law is in progress. The kinetics of the oxidation of hypophosphorous acid by nitric acid will be studied.

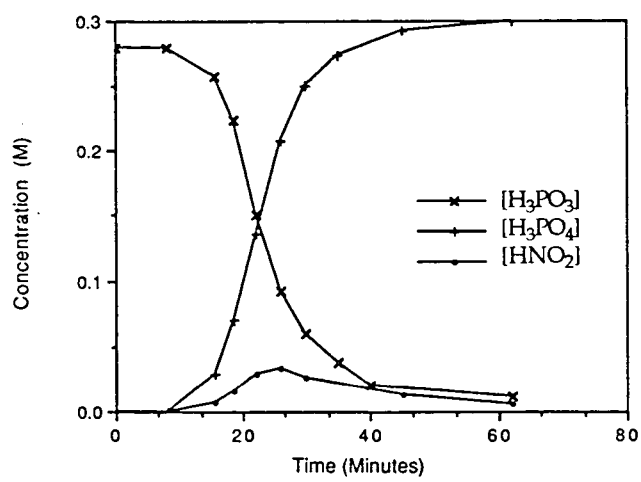

Figure. Oxidation of H_3PO_3 by HNO_3

Developing Advanced Metal Chelates for Removal of NO from Flue Gas

J. B. Zheng and S. G. Chang

Although very efficient in SO_2 removal, the wet limestone flue-gas desulfurization (FGD) system removes little NO_x. This is because most of the NO_x in flue gas is in the form of NO, which is only slightly soluble in aqueous solutions. One approach is to modify the wet limestone FGD system so that NO_x can be removed simultaneously with SO_2 by increasing the solubility of NO. This approach involves addition of metal chelates such as ferrous ethylenediaminetetracetate, Fe^{2+}(EDTA) to the scrubbing liquor to promote the solubility of NO by forming Fe^{2+}(EDTA)(NO). However, several drawbacks occur with the use of Fe^{2+}(EDTA)-type metal chelates. These drawbacks include conversion of NO into N_2O and nitrogen-sulfur compounds, and production of dithionate ion ($S_2O_6^{2-}$). N_2O is a greenhouse gas and will also destroy O_3 in the stratosphere via its photolysis products; $S_2O_6^{2-}$ is very soluble and makes the regeneration of scrubbing liquors for recycling costly.

In view of these drawbacks, we have been developing new metal chelates that would utilize a different scrubber chemistry to prevent the formation of unwanted byproducts. Previously, we developed two new types of ferrous chelates: ferrous thioamino acids/peptides and ferrous dithiocarbamates. Thioamino acids studied include cysteine, acetylcysteine, penicillamine, and acetylpenicillamine; thiopeptides studied include glutathione and cysteinylglycine. The dithiocarbamates investigated are those of iminodiacetate, glycine, diethanolamine, and urea. Most NO is converted to N_2 when ferrous thioamino acids and dithiocarbamates are used. NO is converted to NO_2^- and NO_3^- when ferrous thiopeptides are employed. $S_2O_6^{2-}$ is not produced when the new type of ferrous chelates are used. Despite these improvements, however, none of these ferrous chelates appears to be practical: some are quite sensitive to oxygen, and others are difficult to regenerate after they are oxidized.

We are currently studying the scrubber chemistry of two new ferrous thioamino acid/peptide complexes: N-(2-mercaptopropionyl) glycine (MPG) and L-cysteine ethyl ester (CEE). The oxidation resistance of Fe^{2+}(MPG) and Fe^{2+}(CEE) are better than that of Fe^{2+}(cysteine). With a concentration of Fe^{2+} = 0.01 M and chelate = 0.04 M in a pH 7 solution, and a gas containing 500 ppm NO and 5% O_2, the values for the ratio of number of moles of ferrous ion oxidized per mole of NO removed (n_{Fe2+}/n_{NO}) are 5.5, 4.4, and 20, for MPG, CEE, and cysteine, respectively. The oxidation resistance of the new ferrous chelates is also better than that of Fe^{2+}(EDTA) under the same conditions. The presence of HSO_3^-/SO_3^{2-} in solution appears to slightly improve the (n_{Fe2+}/n_{NO}) ratio. Development of a cost-effective regeneration scheme for the new ferrous chelate systems is in progress.

References

Chang SG, Littlejohn D, Liu D. Use of ferrous chelates of SH-containing amino acids and peptides for the removal of NO_x and SO_2 from flue gas. *IE&C Research* 1988; 27: 2156.

Liu D, Chang SG. Removal of nitric oxide from flue gas using water-soluble iron(II) dithiocarbamates. *Environ. Sci. & Technol.* 1988; 22: 1196.

The Isomers and Dimer of Bisulfite Ion

D. Littlejohn, S.A. Walton, and S.G. Chang

When dissolved in aqueous solutions, sulfur dioxide—a pollutant found in power-plant exhaust gases and in polluted air—can form several species. Complete information on the chemistry of these species is needed to develop efficient flue-gas scrubbing systems and to accurately model atmospheric air pollution. Bisulfite ion, the predominant specie present in pH range 2-7, has two isomeric forms of bisulfite ion present in solution: one isomer has hydrogen bound to the sulfur ion; the other isomer has hydrogen bound to an oxygen atom. Other researchers have measured the equilibrium constant, Q_1,where

$$Q_1 = [HOSO_2^-] / [HSO_3^-].$$

As the concentration of bisulfite ion in solution increases, more of the bisulfite ion dimer, $S_2O_5^{2-}$ (called either pyrosulfite or disulfite ion), is formed. Researchers have not agreed on the equilibrium constant for the formation of $S_2O_5^{2}$, where

$$Q_2 = [S_2O_5^{2-}] / [HSO_3^-]^2.$$

In addition, little is known about formation of $S_2O_5^{2-}$ from the bisulfite ion isomers or about the involvement of $S_2O_5^{2-}$ in the bisulfite ion oxidation process.

We have used Raman spectroscopy to study bisulfite ions in solution over a range of conditions. We studied bisulfite ion solutions with concentration ranging from 0.1 M to 5 M at pH 2-7 at temperatures of 274 to 340 K. These studies permitted us to determine the effect of pH, temperature, S(IV) concentration, and ionic strength on the equilibrium constants Q_1 and Q_2.

Initial temperature-dependent studies showed that the 1023 cm^{-1} Raman peak was associated with $HOSO_2^-$ and that the 1052 and 2530 cm^{-1} peaks were associated with HSO_3^-. Using the areas of the Raman peaks, we calculated the ratios of $HOSO_2^-$ to HSO_3^-; we assumed that the isomers had equal molar scattering efficiency for the 1023 and 1052 cm^{-1} peaks. The ratio obtained indicates that within experimental uncertainty, the two isomers have equal molar scattering efficiency.

With this information, the temperature dependence of Q_1 was determined from spectra of low concentration bisulfite ion solutions ([S(IV)] < 0.3 M).

$$\ln Q_1 = (1458 \pm 152)/T - (3.160 \pm 0.504) \text{ in } H_2O$$
$$= (1567 \pm 79)/T - (3.604 \pm 0.265) \text{ in } D_2O$$

Q_1 does not show any significant dependence on pH over the range of pH 2 to 6 but does show a negative dependence on ionic strength.

Solutions with higher total S(IV) concentrations (in the range of 1-5 M) were studied to determine Q_2, using the $S_2O_5^{2-}$ Raman bands at 235 and 1052 cm^{-1}. The values of Q_2 are tabulated below for H_2O and D_2O at ionic strengths of 1 and 5.

Ionic Strength	H_2O	D_2O
$\mu = 1$	$Q_2 = 0.054 \pm 0.021\ M^{-1}$	$0.028 \pm 0.020\ M^{-1}$
$\mu = 5$	$Q_2 = 0.144 \pm 0.077\ M^{-1}$	$0.13 \pm 0.08\ M^{-1}$

Q_2 showed no significant dependence on pH or temperature, although the data at $\mu = 5$ show it has a negative dependence on the total S(IV) concentration. The measurements of the equilibrium constants will allow determination of the relative concentrations of the various forms of S(IV) in aqueous solutions. They provide some insight into the bisulfite ion reaction processes, although careful studies of the interconversion reactions are needed to provide a complete understanding of the S(IV) chemistry.

— *Atmospheric Aerosols* —

Anomalous SO_2 Oxidation in Laboratory Clouds

A.D.A. Hansen and T. Novakov

Using our mixing-type, continuous-flow laboratory cloud chamber to generate stable, reproducible clouds (composed of 0.2-3 gm^{-3} liquid water), we studied the formation of sulfate when trace quantities of sulfur dioxide and ammonia were introduced into the cloud. This oxidation was found to be much more rapid and complete than could be explained by conventional chemical kinetics models. To investigate the possible role of the nuclei on which the cloud was formed, we used

- sodium chloride and phosphate buffer particles generated from atomized solutions; and
- soot particles from a propane diffusion flame.

No systematic effects were seen, indicating that catalytic or reactive properties of the cloud nuclei were not responsible.

For the oxidation reaction to be observed, the presence of ammonia was necessary; we used a concentration of 1.1 ppm. Because the use of alkaline buffer particles as cloud nuclei did not promote the reaction in the absence of ammonia, we conclude that ammonia plays a chemical role rather than merely increasing the pH of the cloud droplets and the solubility of the sulfur dioxide.

We showed that the reaction did *not* take place in the gas phase, in a dry chamber, as an artifact in the output droplet evaporation/collection systems, or in the same cloud water if collected in bulk and mixed in test tubes.

Varying the contact time between the sulfur dioxide and the cloud from 8 seconds to 3 minutes, we found that the same amount of oxidation was detected. From this we conclude that the reaction is very rapid and probably occurs on the large surface area of the cloud droplets. Using a 0.6-ppm SO_2 concentration in the chamber, we found as much as 80% conversion to sulfate proportional to the cloud liquid water content (Figure). This rate is at least two orders of magnitude greater than would be predicted by kinetics models based on bulk solution results, and we believe that dispersal of the water into the cloud droplet phase may be responsible for this acceleration. This result has far-reaching implications for assessing the effectiveness of emission control strategies on cloud and precipitation acidification.

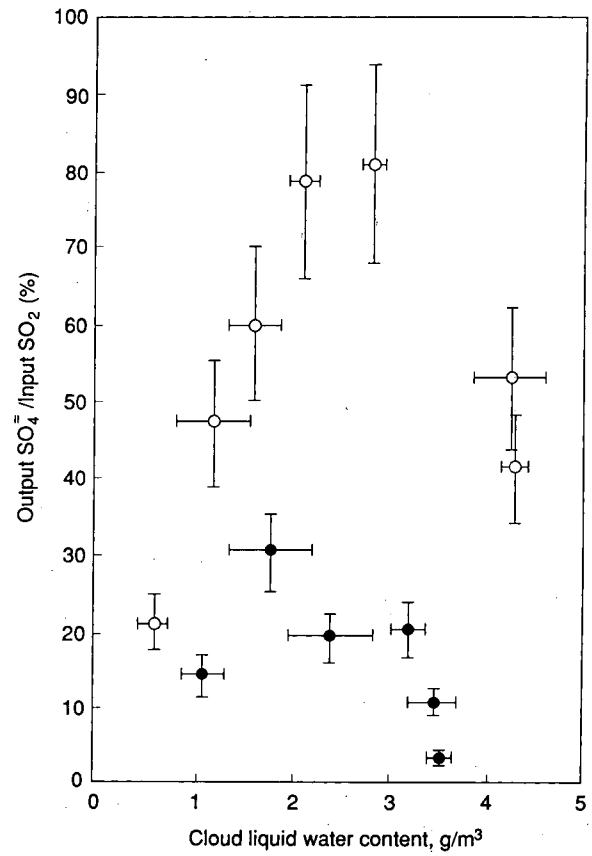

Figure. Results of cloud-chamber studies of anomalous SO_2 oxidation. Percentage of SO_2 shown as a function of cloud liquid water content (LWC). The difference between the two series shown and the decline at high values of LWC is probably attributable to scavenging and losses inside the chamber. Sulfur dioxide-cloud contact time was 3 minutes, and NaCl particles were used as cloud nuclei.
(XBL 8911-4277)

Chemical Characterization of Local and Saharan Dust in the Puerto Rican Atmosphere

R.L. Dod, F. Diaz, R. Giauque, and T. Novakov

We collected daily aerosol samples at the Metropolitan University campus in San Juan, Puerto Rico, from April 1986 to May 1987. An intense Saharan dust episode occurred over the island in April 1987 near the end of this sampling period. The aerosol concentrations during the episode reached very high levels (≥250 mg/m³), greatly exceeding those normally observed in San Juan. This provided us with an opportunity to chemically characterize the dust transported by tradewinds from Africa to Puerto Rico. Earth-moving and construction activity occurred on the campus during 1986, resulting in significant airborne dust during work hours; this enabled us to compare the chemical composition of the local Puerto Rican and Saharan dust.

During most of the sampling program, total aerosol was collected without size segregation. During the second half of the project, however, a dichotomous sampler that collects particles in the "fine" (< 2.5 mm) and "coarse" diameter range (>2.5 mm) was also used. All samples were analyzed by x-ray fluorescence for 26 elements.

The data were analyzed in terms of the "enrichment factor" (EF), defined as EF = (X/A) aerosol/(X/A) crust, where X and A are the concentrations of element X in the aerosol and a global crustal reference element A, such as Al or Fe. If the EF for an element is about 1, it means that its relative concentration in the aerosol is the same as in the crust and that this element is derived exclusively from the soil. EF values much greater than 1 indicate that the element is not crustal and derives either from anthropogenic source or natural sources not originating from the soil. The results of the analyses are shown in the Table; enrichment factors (relative to Fe) are shown for local and Saharan dust for major crustal elements. Coarse and fine fractions of the Saharan dust are also listed.

From the data in the Table, we conclude that Saharan and local dust have similar chemical compositions. We can also see that on the average, 70% of the mass of crustal elements in Saharan dust is confined to particles with aerodynamic diameters greater than 2.5 mm.

The non-crustal elements S, Cl, Se, Br, Sr, and Pb are greatly enriched relative to crustal averages in both Saharan and local dust particles. For these elements, the mass is distributed approximately evenly between coarse and fine fractions.

Element	Local dust	Saharan dust	Fractions in coarse	Fractions in coarse
Al	1.20	1.27	0.66	0.34
Si	0.47	0.50	0.67	-0.33
K	0.52	0.78	0.68	0.32
Ba	0.81	0.42	0.76	0.24
Ti	0.99	1.40	0.72	0.28
V	1.73	1.81	0.70	0.30
Cr	3.25	2.85	0.75	0.25
Mn	1.18	1.22	0.74	0.26
Ni	0.91	0.85	0.64	0.36

Table. Comparison of local Puerto Rican dust and dust transported (by tradewinds) from Africa to Puerto Rico.

High-Velocity Impacts With Submicron-Sized Particles

W.H. Benner and R. Otto

Elemental analysis of individual submicron-diameter particles ($< 5 \times 10^{-13}$ g) is difficult because of the small amount of material available for producing a signal. We have approached this problem by utilizing particle impact ionization, a technique previously used to study the impacts of super-micron cosmic dust particles onto spacecraft detectors. When high-velocity particles ($v > 1$ km/s) strike a suitable target, a fraction of the particle's kinetic energy is converted into ionization energy and produces ions of particle and target constituents. Our continued efforts involve the production of beams of high-velocity particles so that we may study the impact of test particles with metal targets at velocities greater than 1 km/s. Initially, crater formation was observed; we are now progressing toward measurement of ion yields.

Previously, we electrostatically accelerated particles possessing only one unit of charge; we now have accelerated particles charged to their limit. To do so, we developed a particle generator in which a solution is pumped through a small orifice continuously vibrated at ultrasonic frequencies in an electric field. This activity produces droplets of controllable charge; upon evaporation, the droplets leave residual solute particles on which the charge is concentrated. Use of a differentially pumped nozzle-skimmer system produced a beam of these particles and supplied a convenient way to inject the particles into an electrostatic accelerator. We developed instrumentation for studying how the particle beam could be focused; this instrumentation was also used to measure the fractional penetration of the particles through the nozzle-skimmer system.

We studied impacts produced in aluminum targets by particles accelerated through 125 KV. The volume of the observed craters was determined by electron microscopy and is subsequently used in calculations that relate crater volume to target properties and to particle kinetic energy.

We have also designed and begun to construct a device to introduce the charged test particles into a 2-MV van de Graaff accelerator so that greater impact velocities can be studied. These studies will include measurement of ion yields and will move research capabilities toward detecting single-particle events.

— Ecological Systems —

Predicting Chronic Toxicity in Aquatic and Terrestrial Ecosystems

S. Anderson, J. Harte, G. Wild, E. Hoffman, and D. Steward

The effects of environmental pollution and of global ecological change cannot be predicted accurately without further research into the full spectrum of potential effects of low-level, chronic exposures. These effects frequently are not systematically evaluated; in some cases, methods do not exist to predict subtle, sublethal effects. We are currently conducting two projects to predict the effects of chronic exposure to toxic substances in aquatic and terrestrial ecosystems.

In the first project, we have been investigating the potential for toxic effects in marsh habitats of San Francisco Bay. Remarkably, the effects of direct discharges into these marshes have not been characterized, and possibly undesirable effects of marsh reclamation projects throughout the nation remain poorly characterized. We evaluate toxic effects in waters collected from the Bay by conducting laboratory bioassays to determine detrimental reproductive and developmental effects in several species of aquatic organisms, including larval fish and marine invertebrate embryos. Marsh sites are selected so as to assess the potential detrimental effects of domestic and industrial wastewater, as well as urban runoff.

We have observed toxic effects in two marshes. In one marsh receiving treated municipal wastewater, water from three of six ponds was acutely toxic to fish and to crustacean test species. Some toxicity is attributable to non-ionized ammonia, but additive effects of other toxic substances appear to be causing more widespread toxicity. For another marsh, we documented subtle sublethal effects of both treated municipal effluent and urban runoff. Interestingly, samples from one marsh area receiving more than 50 million gallons of treated municipal wastewater daily caused no toxic effects in the laboratory bioassays. We are doing additional work to determine whether subtle toxic effects observed at some reference stations are attributable to elevated concentrations of trace metals.

Our second project aims to determine the value of incorporating genetic toxicology into ecological risk assessment. Substances that affect genetic material may cause decreased fertility, cancer, and mutations in subsequent generations; however, these effects cannot be predicted using existing assessment techniques. Our recent efforts have centered on developing and validating a genotoxicity bioassay using the nematode *Caenorhabditis elegans*. More than a thousand mutants of this species have been isolated, and for many of these mutants, affected genes have been mapped. Because this type of basic genetic information is available to us, well-characterized dominant and recessive lethal mutants can be recovered in any of a variety of possible screens. We recently completed one of the screens successfully, mutants having been identified using the reciprocal translocation eT1(III, V). The recessive lethal mutants were identified in 10 days and were confirmed in 15 days. We are evaluating the sensitivity of three possible screens using three types of mutants and strains known to be DNA-repair deficient. The sensitivity and selectivity of these screens will be evaluated in comparison to that of other mutagenesis assays and assays of reproductive and developmental effects in fish and invertebrates such as those that are used in the San Francisco Bay project.

During 1990, the nematode assay will be used to pursue research into the genotoxic effects of increasing UV exposure as a consequence of stratospheric ozone depletion. In this research, we will investigate effects in wild-type and UV-sensitive strains and will develop population models to describe potential population-level changes that may occur in response to increasing mutation rates. (In this case, the nematode is used not because it is an indicator species for affected sites, but because the basic genetics of DNA modification and repair can be evaluated.) This effort illustrates the ongoing goal of our group: to combine environmental modelling and toxicology in addressing the effects of global ecological change and environmental contamination.

Reference

Anderson SL, Harrison FL. Predicting the ecological significance of exposure to genotoxic substances in aquatic organisms. In: S. Saudhu, ed., *First Symposium on In Situ Evaluation of Biological Hazards of Environmental Pollutants.* Plenum Press, N.Y.

— *Membrane Bioenergetics* —

Detecting and Preventing Biological Free-Radical Damage

R.J. Mehlhorn, J. Maguire, K. Moore, T. Prolla, J. O'Neill-Gonzalez, and L. Packer

Because of recent progress in detecting biological free-radical damage, researchers can demonstrate the ubiquity of this damage. Understanding its basis and how it might be ameliorated is now recognized as a major opportunity in biological research, with profound implications for human welfare—including prevention of major diseases and extension of lifespans. The Membrane Bioenergetics Group has pioneered methods to detect free radicals and applies these methods to studying the mechanisms of free-radical reactions and the processes that have evolved to protect cells from oxidative damage.

Our research aims to elucidate mechanisms of free-radical production and antioxidant action, including how vitamins C and E protect animals against free radicals. Our principal experimental approach in this work is *electron spin resonance* (ESR), which detects magnetic moments present in all free radicals. This basic approach is rendered highly sensitive with *free-radical traps*, which accumulate products of free radical reactions. We are also developing a new chemical method whose basis is a radiolabeled chemical (that can be injected into an animal) whose reaction with hydroxyl and other strongly reactive oxyradicals causes it to decompose into several fragments, including a small radiolabeled hydrocarbon fragment that is volatilized in the lung and detected in expired breath.

STUDIES OF THE VITAMIN E RADICAL

New ESR methods we have developed have enabled us to investigate how the alpha-tocopheroxyl radical interacts with chemical and enzymic reducing agents. We found vitamin C to be an effective reductant, whereas uric acid was ineffective. Electron transport activity of subcellular liver membranes was also shown to regenerate vitamin E, thus allowing it to act as a catalytic free-radical scavenger. We therefore believe it likely that, the reducing agents involved in recycling vitamin E may be as important in protecting membranes from free radical damage as the dietary intake of this vitamin.

ASCORBATE RECYCLING MECHANISMS

We have developed a new ESR assay for vitamin C and have applied it to the human erythrocyte. This assay showed that ascorbic acid is enzymically recycled. In conjunction with glutathione reductase, the pentose phosphate shunt efficiently regenerates ascorbic acid from dehydroascorbic acid. Hydroperoxide inhibits this reduction pathway, providing new insight into peroxide toxicity mechanisms.

MECHANISM OF ACTION OF A DRUG THAT INDUCES CHEMICAL PARKINSONISM

To understand the role of mitochondrial energy inhibition in chemically-induced Parkinson's disease, we used ESR methods to help establish that 1-methyl-4-phenylpyridinium ion (MPP^+) exerts a potent inhibitory effect on mitochondrial NADH dehydrogenase by binding to a hydrophobic intramembranous site of the enzyme.

Free Radicals in Skin

Skin manifests some of the most familiar aging symptoms, and excessive exposure to sunlight is well known to correlate with the early appearance of some aging markers. We have conducted ESR studies of free radicals in epidermis and skin homogenates. We characterized the free-radical reducing activity of a) isolated thioredoxin reductase, a flavin containing oxidoreductase, b) skin homogenates, and c) the epidermis of hairless mice. We concluded that the epidermis contains an effective antioxidant system that scavenges ascorbate-sensitive nitroxides as well as more reducing radicals such as dihydropyrroloxy nitroxides.

Production of Free Radicals by Thyroid Peroxidase

Peroxidase enzymes are well known to generate powerful oxidants *in vitro*. We have discovered that ESR measurements of the oxidation of the reduced nitroxide TOLH can be used to accurately measure hydrogen peroxide, peroxidase activity, and phenols present in tissue homogenates. Applying this assay to thyroid preparations from a variety of animals, we have demonstrated free-radical production by peroxidase enzymes with an exogenous source of hydrogen peroxide (glucose oxidase and glucose) and several phenols. The availability of this enzymic free-radical source has been a key to our success in detecting free radicals derived from vitamin E. We have also discovered that TOLH is a powerful antioxidant that protects cultured thyroid cells from the lethality of exogenous free radicals. We are currently attempting to assess the efficacy of TOLH in other biological systems.

References

Mehlhorn RJ, Sullivan R. Measurement of bioenergetics phenomena in cyanobacteria with magnetic resonance methods. *Methods Enzymol.* 1988; 167:509-518.

Belkin S, Mehlhorn RJ, Packer L. Electron spin resonance oximetry. *Methods Enzymol.* 1988; 167:670-677.

Dragutan I, Dragutan V, Mehlhorn RJ. Convenient synthesis of spin labeled amines. *Bull. Soc. Chem.* Belg. 1988; 97:457-459.

Dragutan I, Caldararu H, Balaban AT, Mehlhorn RJ. *Bull Soc. Chem.* Belg. 1988; 97:453-455.

Todd AP, Mehlhorn RJ, Macey RI. Amine and carboxylate spin probe permeability in red cells. *J. Membane Biol.* 1989; 109:41-52.

Packer L, Maguire J, Mehlhorn RJ, Serbinova E, Kagan VE. Mitochondria and microsomal membranes have a free radical reductase acitvity that prevents chromanoxyl radical accumulation. *Biochem. Biophys. Res. Comm.* 1989; 159:229-235.

Mehlhorn RJ, Sumida S, Packer L. Tocopheroxyl radical persistence and tocopherol consumption in liposomes and in vitamin E-enriched rat liver mitochondria and microsomes. *J. Biol. Chem.* 1989; 264:13448-13452.

Ramsay RR, Mehlhorn RJ, Singer TP. Enhancement by tetraphenylboron of the interaction of the 1-methylphenylpyridinium ion (MPP^+) with mitochondria. *Biochem. Res. Commun.* 1989; 159:983-990.

Mehlhorn RJ, Fuchs J, Sumida S, Packer L. Preparation of tocopheroxyl radicals for detection by ESR. *Methods in Enzymol.* (in press)

Fuchs J, Mehlhorn RJ, Packer L. Free radical reduction mechanisms in mouse epidermis and skin homogenates. *J. Invest. Dermatol.* 1989; 93:633-640.

Prolla T, Mehlhorn R. A photochemical system for generating free radicals: Superoxide, phenoxyl, ferryl and methyl. *Free Rad. Res. Commun.* (in press, 1989)

— *Analytical Chemistry* —

Asteroid Impacts on the Earth

F. Asaro, H.V. Michel, and W. Alvarez

The relation between the impact of a large asteroid or comet (10 km in diameter) on the Earth and the worldwide distribution of a 65 million-year-old layer of Iridium-enriched sediments has been amply documented and is widely accepted; the relation between the impact and the extinctions of many species has also been amply documented but is not as widely accepted. More controversial are studies suggesting that the extinctions of species were periodic and were related to periodic astrophysical phenomena. Our project tests the periodicity of the impact of large asteroids or craters on the Earth and examines the relation to extinctions.

The technology of our Iridium Coincidence Spectrometer has been significantly improved: the instrument now can simultaneously analyze 13 other elements in samples and can measure very low levels of iridium after neutron activation. We have also found a second section (Ocean Drilling Program Core ODP 689B, 6H3, 50-60 cm) from the Maude Rise of Antarctica which has an iridium anomaly (possibly impact-related) in sediments 10-12 million years old (i.e., of the Middle Miocene period).

In another core (14H-6, 100-110 cm) from the same hole, we found a single iridium anomaly of 155 ppt—over a background of 7 ppt—in sediments 35-39 million years old (i.e., of the Late Eocene). Approximately 64° south latitude, this is the most southern extension of this anomaly and helps confirm the worldwide distribution of this impact-related iridium anomaly in the southern hemisphere.

Possibly four stratigraphic levels of iridium-enriched rocks have now been discovered, deposited approximately 10-12, 35-39, 65-67, and 91-92 million years ago. Two of these levels are likely to be related to impacts; the first is probably related, and the origin of the last is uncertain. If all these levels are related to impacts, the data suggest a periodicity of approximately 27 million years.

Proposed by our group and performed jointly with several laboratories, an intercalibration study is examining splits of an identical sampling of a level 1.8 meters below the Italian Cretaceous-Tertiary (K-T) boundary. This study was designed to settle a serious dispute as to the true iridium content. An intensive search for Late Eocene iridium anomalies (35-39 million years old) in the Eocene-Oligocene Type section at Massignano, Italy, is also being performed using precise stratigraphic controls. This study may help determine the northern extension of the Late Eocene anomaly. We hope to complete a detailed study of rocks between 65 and 91 million years old to determine whether the iridium anomalies we have observed are unique.

This document was prepared as an account of work sponsored by the United States Government. Neither the United States Government nor any agency thereof, nor The Regents of the University of California, nor any of their employees, makes any warranty, express or implied, or assumes any legal liability or responsibility for the accuracy, completeness, or usefulness of any information, apparatus, product, or process disclosed, or represents that its use would not infringe privately owned rights. Reference therein to any specific commercial product, process, or service by its trade name, trademark, manufacturer, or otherwise, does not necessarily constitute or imply its endorsement, recommendation, or favoring by the United States Government or any agency thereof, or The Regents of the University of California. The views and opinions of authors expressed herein do not necessarily state or reflect those of the United States Government or any agency thereof or The Regents of the University of California and shall not be used for advertising or product endorsement purposes.

Lawrence Berkeley Laboratory is an Equal Opportunity Employer

Applied Science Division
Lawrence Berkeley Laboratory
University of California
Berkeley, CA 94720